Machine-related backgrounds in the SiD detector at ILC

D.S. Denisov, N.V. Mokhov and S.I. Striganov

Fermilab,
P.O. Box 500, Batavia, IL 60510, U.S.A.
E-mail: strigano@fnal.gov

M.A. Kostin

NSCL, Michigan State University,
East Lansing, MI 48824, U.S.A.

I.S. Tropin

Tomsk Polytechnic University,
Tomsk, 634034, Russia

ABSTRACT: With a multi-stage collimation system and magnetic iron spoilers in the tunnel, the background particle fluxes on the ILC detector can be substantially reduced. At the same time, beam-halo interactions with collimators and protective masks in the beam delivery system create fluxes of muons and other secondary particles which can still exceed the tolerable levels for some of the ILC sub-detectors. Results of modeling of such backgrounds in comparison to those from the e^+e^- interactions are presented in this paper for the SiD detector.

KEYWORDS: Instrumentation for particle accelerators and storage rings - high energy (linear accelerators, synchrotrons); Detector modelling and simulations I (interaction of radiation with matter, interaction of photons with matter, interaction of hadrons with matter, etc); Large detector systems for particle and astroparticle physics.

Contents

1. Introduction

The collimators of the International Linear Collider (ILC) Beam Delivery System (BDS) are intended to localize the beam loss in dedicated regions far from the Interaction Point (IP) to substantially reduce backgrounds in the collider detectors [1]. Particle fluxes resulting from the interactions of beam halo with the collimators, protective masks and other limiting apertures could still exceed tolerable levels for some of the ILC sub-detectors. Magnetic spoilers in the tunnel can reduce muon fluxes substantially [2]. Response of the Silicon Detector (SiD) sub-detectors [3] to these backgrounds is calculated and presented in this report.

2. BDS and detector models, scraping rate and beam parameters

Following the SLAC Linear Collider (SLC) experience, it is assumed that the ILC collimation system cuts 0.1% of the beam outside of a predefined beam envelope. Such scraping rate at the SLC could be explained by absence of pre-linac collimation and by tails coming from the dumping rings. Using the same loss rate in the ILC BDS seems to be conservative, but it is accepted at the present stage as a specification for the collimation system and BDS designs [1, 4]. Details of the BDS and collimation system designs and calculated beam loss distributions in the region are described elsewhere [1, 5, 6].

Beam losses in the BDS are simulated with the STRUCT code [7]. Starting from beam loss distributions on the betatron and momentum spoilers SP2, SP4, SPEX, full 3-D shower simulations through the entire 1.8-km long BDS system are performed with the MARS15 code [8]. A sketch of the ILC collimation system layout used in the calculations is presented in figure 1. The MARS15 model of the BDS includes all the primary collimators (spoilers), absorbers, protection collimators,
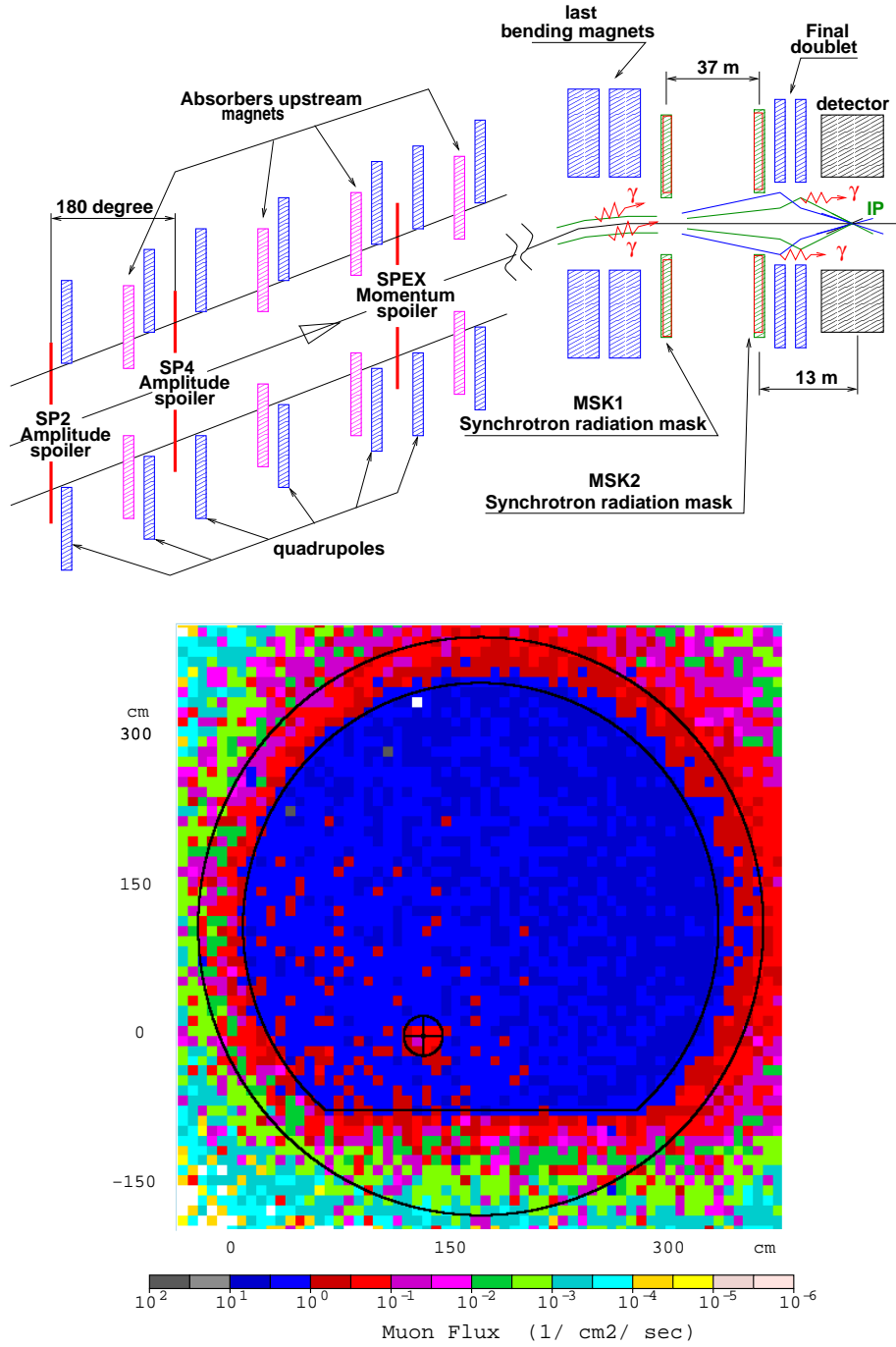
Figure 1. BDS layout (top) and muon flux at the tunnel-experimental hall transition (bottom).

synchrotron radiation masks, focusing and bending magnets with proper materials, 3-D geometry and magnetic fields, tunnel walls and surrounding dirt [1]. These calculations provide particle parameters and tagging information with the cutoff energy of 0.1 MeV at the entrance to the detector.

Barrel	Inner radius (cm)	Outer radius (cm)	Inner Z (cm)	Outer Z (cm)
Vertex detector	1.4	6	0	6.25
Tracker	20	121.3	0	161.7
Ecal	127	138.25	0	179.5
Hcal	138.5	233.7	0	277
Muon system	333	645	0	277
Endcap	Inner radius (cm)	Outer radius (cm)	Inner Z (cm)	Outer Z (cm)
Vertex detector	1.6	7.5	7.6	18
Tracker	4	126.3	30	165.4
Ecal	26	126.5	168.1	179.25
Hcal	26	138.25	179.5	274.7
Muon system	26	645	277.5	589.5
LumCal	2	14.28	295	313.75
FEcal	8.69	25	168	179.25

Table 1. SiD sub-system dimensions.

The source of the muon component of BDS backgrounds is concentrated in the collimation region 800 to 1500 m from the IP. Muon flux from this source on the detector can be substantially reduced by massive magnetic steel blocks in the tunnel closer to the experimental hall [9]. With two spoilers 9 and 18-m long at 648 and 331 m from the IP, the muon fluxes at the detector can be reduced by a few thousand times, as was shown with the MUCARLO and MARS15 codes [2]. Each muon spoiler consists of two steel parts with magnetic coils which provide the opposite field polarities in order to compensate field in the beam pipe. The magnetic field in the iron is 1.5 T. The gap between the parts accommodates the beam pipe. The winding slots in the center of each iron part are 10-cm wide and 1-m high with a field of about 0.8 T. They are assumed empty in this study. The spoilers are extended into the tunnel wall/dirt by 60 cm horizontally to prevent muon backscattering. The spoiler geometry, magnetic field distribution as well as simulated particle tracks in the spoiler region — as modeled with MARS15 — are shown in figure 2. The calculations are performed for two cases: with and without muon spoilers in the BDS tunnel.

SiD detector response is calculated using the Simulator for the Linear Collider (SLIC) and its geometry package, Linear Collider Detector Description (LCDD). LCDD includes various detector configurations, such as SiD, GLD, TESLA(D09) and others [10]. Simulations in this paper are performed using the Silicon Detector (SiD) geometry. SLIC takes into account a detailed description of the SiD geometry, the magnetic field and sensitivity of different sub-systems. Dimensions of the SiD sub-detectors are presented in table 1. SLIC provides possibility to calculate time and space distributions of hits in the detector. The SiD LCDD description includes 12 detector sub-systems. "Calorimeter" type hits are simulated in the Muon Endcap and Barrel, Hcal Endcap and Barrel, Ecal Endcap and Barrel, ForwardEcal Endcap and Luminosity Monitor. "Tracker" hits are simulated for tracker (Endcap and Barrel) and vertex (Endcap and Barrel) detectors. The "calorimeter" hit information is quantized into cells in the GEANT4 program. The total energy deposited (and time of deposition) by each primary particle in a calorimeter cell is recorded. This, however, is done at a finer segmentation than is expected to be available in a real detector. A "real" number of
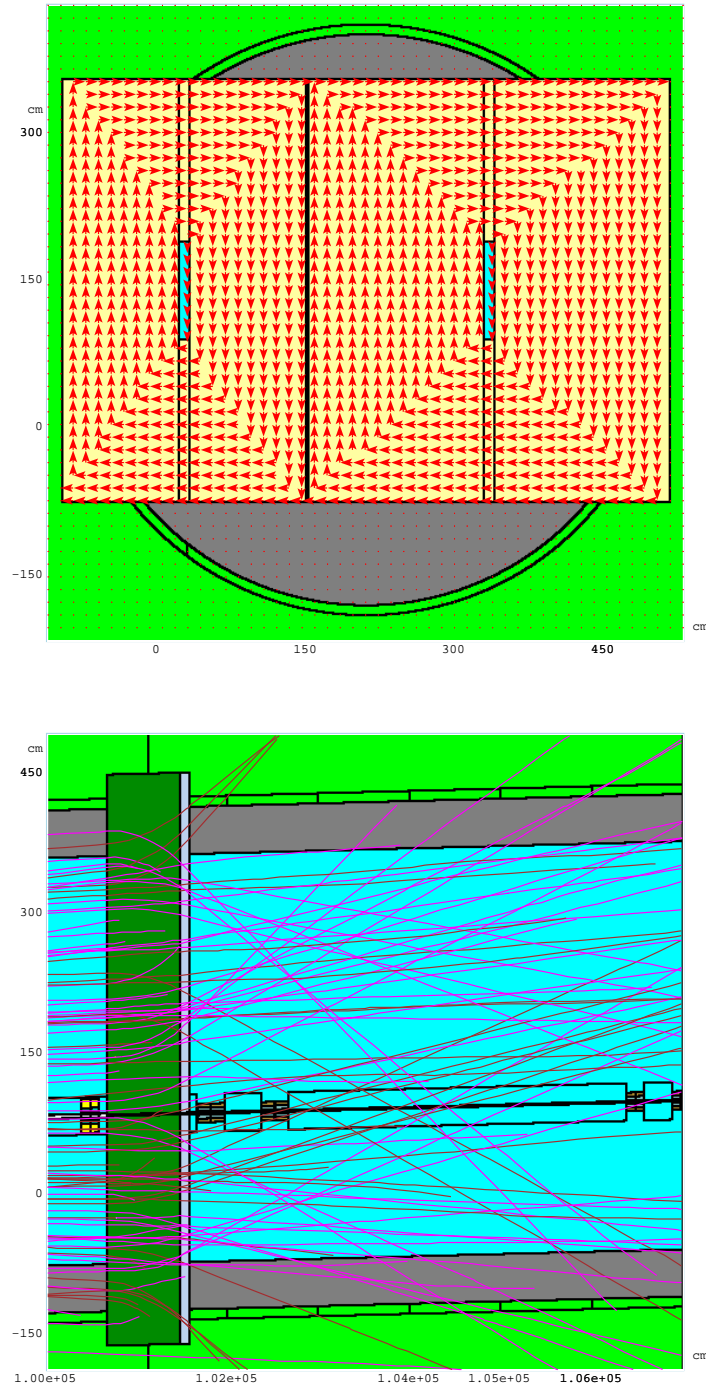
Figure 2. MARS15 muon spoiler with magnetic field lines (top) and muon tracks in the spoiler region (bottom).

hits could be lower if realistic segmentation and thresholds are taken into account. It could be done when details of the detector geometry are finalized.

	γ	$\mu^{\pm}$	e^+	e^-	neutron
With spoilers	2927	0.024	1172	$3.6\cdot10^{-4}$	6364
No spoilers	2942	60.4	1095	10	346

Table 2. Average number of particles per bunch at the SiD from positron tunnel.

	γ	$\mu^{\pm}$	e^+	e^-	neutron
with spoilers	$5.4\cdot10^{-3}$	38	251	0.13	$1.6\cdot10^{-3}$
no spoilers	$5.5\cdot10^{-3}$	28	250	0.19	$7\cdot10^{-4}$

Table 3. Average kinetic energy (GeV) of particles at the SiD from positron tunnel.

The nominal ILC beam parameters [11] are used in this study: the beam consists of 5 trains per second with 2820 bunches in each train, time between trains is 199 ms, the train length is 868 μs. There are 2×10^{10} positrons/electrons in each bunch and the luminosity is 2×10^{34} cm^{-2} s^{-1}.

3. BDS induced detector backgrounds

The spoilers drastically reduce muon and electron fluxes at the detector. The BDS-induced muon flux averaged over the tunnel cross-section at the entrance to the experimental hall is 4.1 cm$^{-2}s^{-1}$ without spoilers, while it is 1.2×10^{-3} cm$^{-2}s^{-1}$ with the spoilers described in the previous section. Note that the effect of muon penetration through the central gap and holes in the left/right parts is quite substantial: filling them with steel reduces the above flux by a factor of three, resulting in a shielding effect of such hypothetical spoilers of a factor of 10^4. Filling/screening of these openings (at least partial) to reduce further backgrounds in the detector and radiation levels the experimental halls should be considered in the future.

Average number of background particles produced by the positron beam and their average energy at the Muon Endcap (589 cm from the IP) are presented in tables 2, 3. Energy spectra of background particles are shown in figure 3. Average number and energy of photons and positrons are practically not changed by the spoilers. Most of photons and positrons are coming near or inside the beam pipe while radial distributions of other particles are rather flat over the first three meters from the beam axis (see figure 4). Based on a limited statistics for neutrons, their flux rises about 20 times with the spoilers installed. The neutrons coming from the tunnel are not a serious concern at this stage, because it is envisioned that there will be standard concrete wall plugging the tunnel at the entrance to the experimental hall which will absorb most of the BDS neutrons. Similar machine-induced backgrounds irradiate the other side of the detector from the electron beam.

There is also the IP-related background in the detector, e^+e^- pairs and radiative Bhabhas from beam-beam interactions [2]. Maruyama [12] has calculated responses of the vertex and tracker SiD sub-detectors to these backgrounds using the GEANT3 and Guineapig programs. These backgrounds depend on the beam crossing angle. The IP-related background could be reduced using a low-Z masks in the detector. The 20-mrad option with a low-Z shielding is selected for comparison with calculations presented in this report. The BDS-induced background hit rates are compared with hits produced by electron-positron interactions in the IP. Secondary particles from
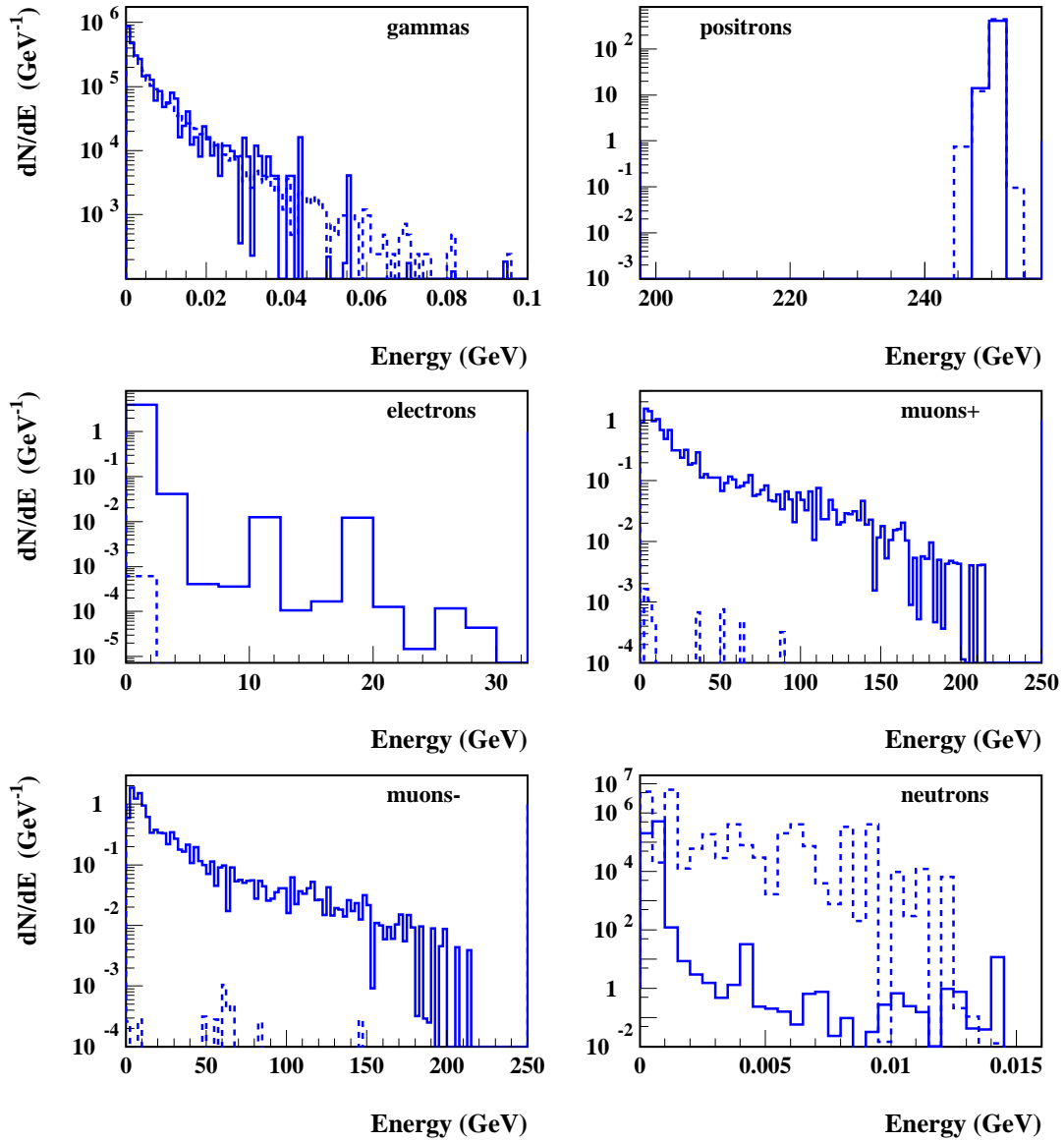
Figure 3. Energy spectra of particles at the SiD detector (per bunch). Solid line - no spoilers, dashed line - tunnel with spoilers. Particles come from positron tunnel only.

250×250 GeV e^+e^- collisions are simulated using the PYTHIA code [13] with a cross-section of 1.8×10^{-8} mb. The detector response for these particles is calculated using the SLIC code.

4. Hit rates in sub-detectors

Hit rates in SiD detector sub-systems from the positron tunnel, IP backgrounds and e^+e^- events are presented in figure 5. Background from the tunnel (no spoiler option) produces much more hits in the muon system than e^+e^- interactions in the IP. The BDS-backgrounds (without spoilers) and e^+e^- collisions give almost identical hit rates in the hadronic calorimeter. The spoilers reduce the
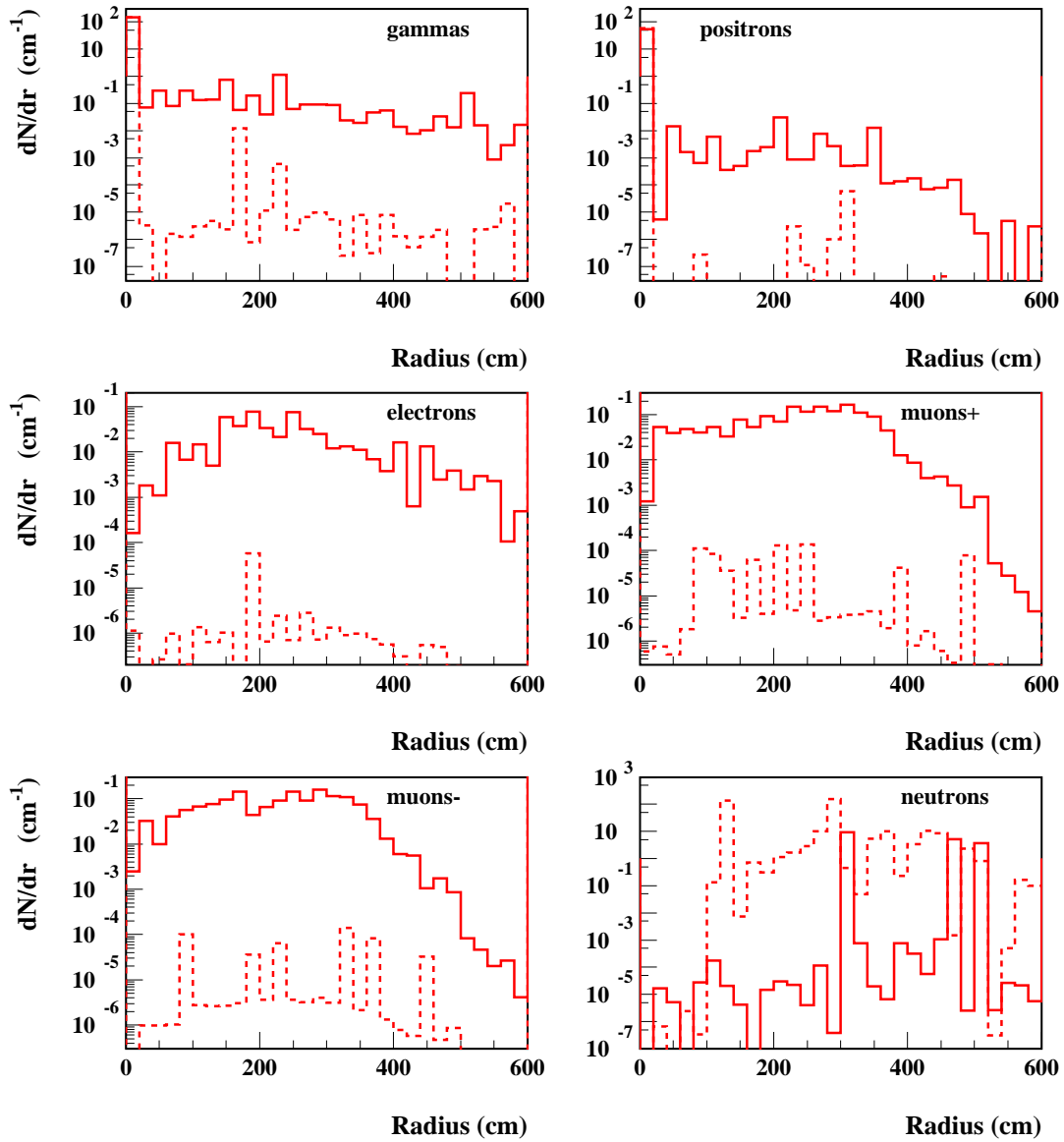
Figure 4. Radial distributions of particles at the SiD detector (per bunch). Solid line - no spoilers, dashed line - tunnel with spoilers. Particles come from positron tunnel only.

rates in these sub-detectors by more than three orders of magnitude. In all other sub-detectors, the e^+e^- contribution dominates.

The muon spoilers reduce the BDS-induced backgrounds in most of the sub-systems. The only exception is the vertex detectors where the effect is opposite, although this conclusion is based on a low statistics for these sub-detectors. The effect of spoilers should be negligible there, because the main source of the tunnel background for vertex detectors is near-beam positrons and photons. These positrons are due to the beam halo "quasi-elastic" scattering in the collimator jaws. They pass the spoilers within the beam pipe. The related photons are created after the spoilers. Therefore,
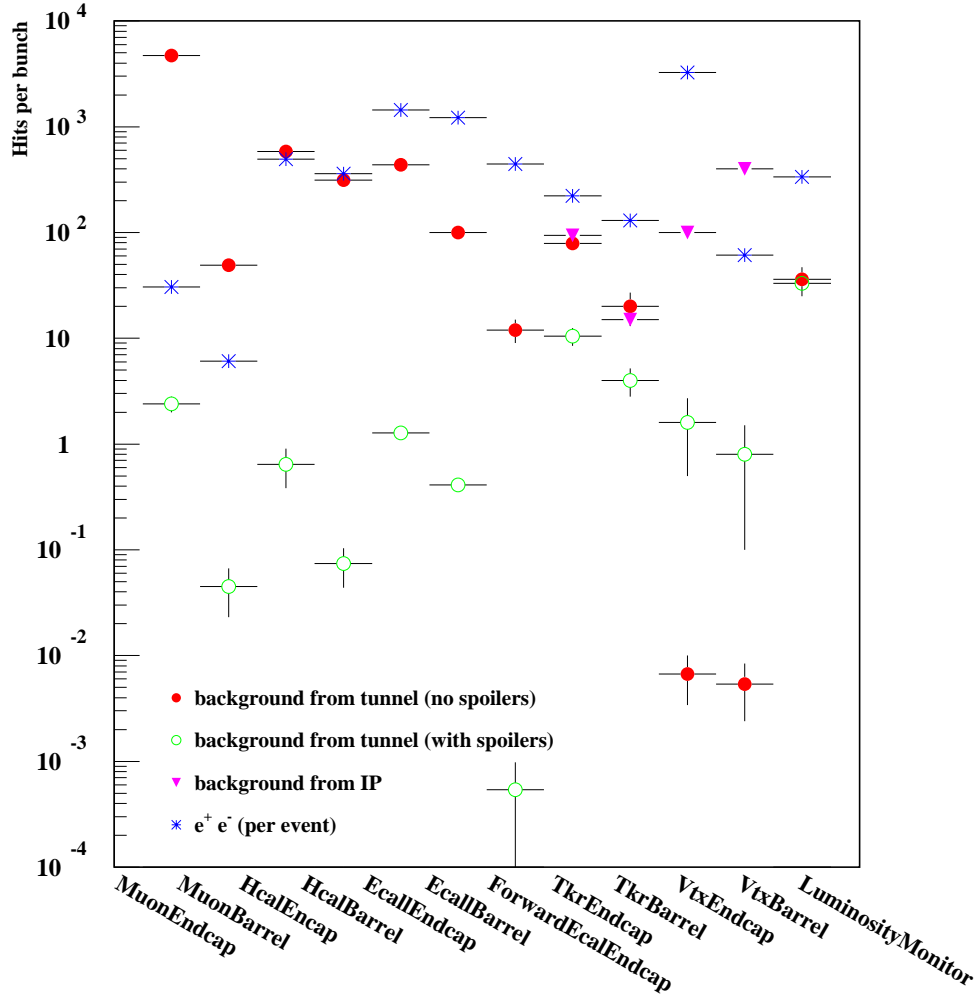
Figure 5. Hit rates in detector sub-systems. Tunnel background is created by particles coming from positron tunnel only.

the numbers and spectra of these particles in the near-beam region at the IP (vertex detectors) are practically not affected by the tunnel spoilers (see tables 2, 3 and figures 3–4). As seen from figure 5, the IP-induced backgrounds dominate the vertex Endcap and Barrel occupancies.

A statistical uncertainty of neutron-produced hit rates is substantial. At this stage, the details that drive the neutron fluxes in the ILC detectors — configuration, dimensions and materials of the experimental hall and tunnel interface, passive materials of the calorimeters — are quite uncertain. There are also concerns about accuracy of the current SLIC/GEANT4 simulation of low-energy neutron transport [15].

Hit rates for the BDS backgrounds are presented in tables 4, 5. Muons are the main source of the machine backgrounds for the SiD except luminosity monitor. Most of the muons have enough energy to pass through the whole detector (see figure 6). They move perpendicularly to the sensitive layers of the Endcaps (Muon, Hcal, Ecal, FEcal). Therefore, every muon produces about one hit in

	All hits/bunch	γ %	$\mu^{\pm}$ %	e^+ %	e^- %	neutron %
Muon Endcap	4711	0.2	99.4	0.1	0.3	0
Muon Barrel	49	0	100	0	0	0
Hcal Endcap	584	0	100	0	0	0
Hcal Barrel	314	0	100	0	0	0
Ecal Endcap	435	0	100	0	0	0
Ecal Barrel	100	0	100	0	0	0
FEcal Endcap	12	0	100	0	0	0
Tkr Endcap	79	0	95	5	0	0
Tkr Barrel	20	59	41	0	0	0
Vtx Endcap	$6.7 \cdot 10^{-3}$	0	100	0	0	0
Vtx Barrel	$5.4 \cdot 10^{-3}$	0	100	0	0	0
Luminosity Monitor	36	45	10	45	0	0

Table 4. Contribution of particles from the positron tunnel to hit rates in the SiD sub-detectors without spoilers.

	All hits/bunch	γ %	$\mu^{\pm}$ %	e^+ %	e^- %	neutron %
Muon Endcap	2.4	0	99	0	0	1
Muon Barrel	0.045	0	100	0	0	0
Hcal Endcap	0.642	0	100	0	0	0
Hcal Barrel	0.074	0	100	0	0	0
Ecal Endcap	1.28	62	38	0	0	0
Ecal Barrel	0.41	98.4	1.6	0	0	0
FEcal Endcap	$5.4 \cdot 10^{-4}$	0	100	0	0	0
Tkr Endcap	10.5	72.5	0.7	26.8	0	0
Tkr Barrel	4	70	0	30	0	0
Vtx Endcap	1.6	100	0	0	0	0
Vtx Barrel	0.8	0	0	100	0	0
Luminosity Monitor	36	35	0	65	0	0

Table 5. Contribution of particles from the positron tunnel to hit rates in the SiD sub-detectors with spoilers.

a sensitive layer of the Endcaps. Total hit number N_{hit} in the Endcaps can be estimated as

$$N_{\text{hit}} = \int_{r_{\text{min}}}^{r_{\text{max}}} dr f_\mu(r) \cdot N_{sl}, \qquad (4.1)$$

where $f_\mu(r)$ is the radial distribution of incoming muons (figure 4), r_{min} and r_{max} are the minimal and maximal radii of the Endcap, and N_{sl} is a number of sensitive layers. The tracker Endcap is the special case. It consists of two sub-systems, 5 layers each, and every layer has different minimal
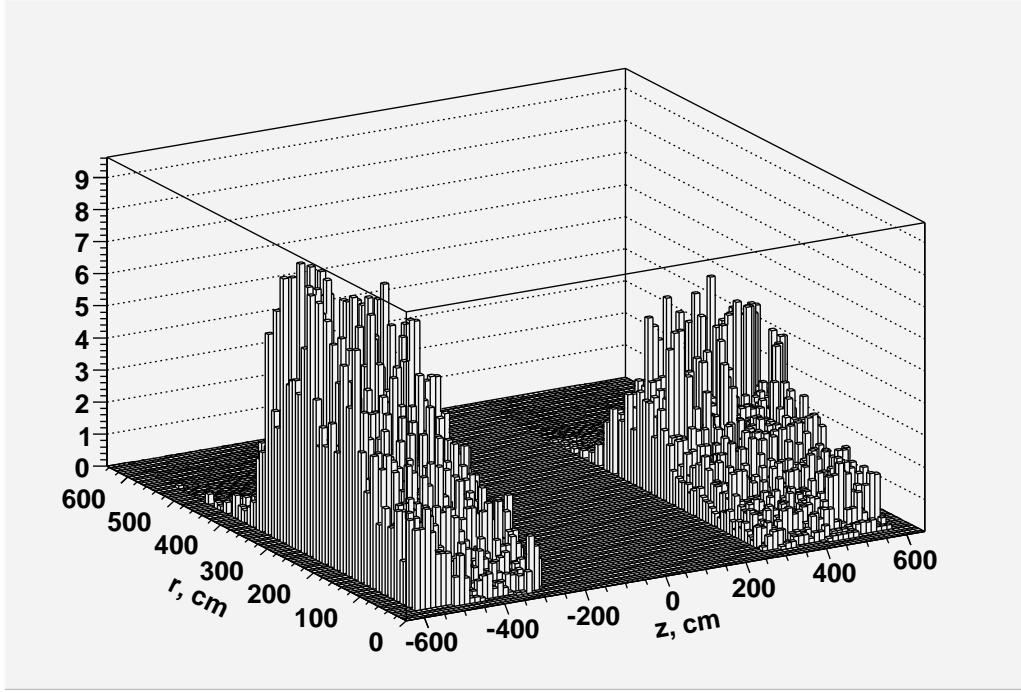
Figure 6. RZ distribution of hits per bunch in Muon Endcap. No spoilers. Background is created by particles coming from positron tunnel only.

	spoilers	N muons $r^{\min} < r < r^{\max}$	N layers	muon hits (1)-(2)	muon hits simulation	all hits simulation
Muon Endcap	no	60.4	48·2	5798	4685 ± 160	4711
Hcal Endcap	no	10.7	34·2	725	584 ± 50	584
Ecal Endcap	no	9.5	30·2	568	435 ± 43	435
FEcal Endcap	no	0.078	30·2	4.7	11.7 ± 4.6	11.7
Tkr Endcap	no	23	(5)2·2	92	75 ± 10	79
Lum Monitor	no	0.024	50·2	2.4	3.9 ± 2.5	36
Muon Endcap	yes	0.024	48·2	2.3	2.4 ± 0.6	2.4
Hcal Endcap	yes	$6.8 \cdot 10^{-3}$	34·2	0.46	0.64 ± 0.28	0.64
Ecal Endcap	yes	$6.8 \cdot 10^{-3}$	30·2	0.41	0.48 ± 0.22	1.28
FEcal Endcap	yes	$2.2 \cdot 10^{-5}$	30·2	$1.3 \cdot 10^{-3}$	$5.4 \cdot 10^{-4} \pm 4.4 \cdot 10^{-4}$	$5.4 \cdot 10^{-4}$
Tkr Endcap	yes	0.013	2·2	0.052	0.078 ± 0.040	10.5
Lum Monitor	yes	$1.3 \cdot 10^{-5}$	50·2	$1.3 \cdot 10^{-3}$	$3.4 \cdot 10^{-4} \pm 2.1 \cdot 10^{-4}$	36.

Table 6. Comparison between simple model (1)-(2) and simulation.

and maximal radii. There are two detection planes in each layer. In this case

$$N_{\text{hit}} = 2 \times 2 \times \sum_{n=1}^{5} \int_{r_{min(n)}}^{r_{max(n)}} dr f_\mu(r). \tag{4.2}$$

A comparison of simulation and a simple model (1)-(2) is shown in table 6. The model agrees with the SLIC simulations of muon hits in the Endcaps within about 20%. This model can be used to estimate hit rates in the Endcaps for different Endcap designs.

– 10 –

	Sensitive area cm^2	Hit number per bunch	occupancy per bunch
Muon Endcap	$1.3 \cdot 10^8$	$4711 \cdot 2$	0.008 %
Muon Barrel	$8.2 \cdot 10^7$	$49 \cdot 2$	0.0001%
Hcal Endcap	$3.9 \cdot 10^6$	$584 \cdot 2$	0.03 %
Hcal Barrel	$2.2 \cdot 10^7$	$314 \cdot 2$	0.003 %
Ecal Endcap	$2.9 \cdot 10^6$	$435 \cdot 2$	0.03 %
Ecal Barrel	$9.0 \cdot 10^6$	$100 \cdot 2$	0.002 %
FEcal Endcap	$1.0 \cdot 10^5$	$12 \cdot 2$	0.02 %
Lum Monitor	$6.3 \cdot 10^4$	$36 \cdot 2$	0.12 %

Table 7. Tunnel background occupancies in sub-detectors (no spoilers) taking into account both electron and positron beam losses.

5. Tolerable limits and machine backgrounds

Possible approach to the tolerable background levels in different ILC detector sub-systems was discussed in ref. [14]. For calorimeter, tracker and vertex detectors, a limit on a background occupancy was estimated to be about 1%. A segmentation of the SiD calorimeters is not finalized yet. Using a cell size of 1 cm^2 and table 4, the background occupancy for the calorimeters could be estimated. Results are presented in table 7 and can be simply re-scaled to another cell size. The occupancy levels are smaller than 1% if the detector integration time is shorter than a time between bunches.

An estimate of acceptable background levels in the SiD tracker has also been presented in ref. [14]. To avoid a pattern recognition problem, the hit density from charged particles should be lower than 0.2 hit/cm^2/bunch. To avoid a pile-up problem, the background level should be lower than 0.2 hit/mm^2/train. The calculated tunnel-related background distributions in the Tracker Endcap and Barrel are rather flat (see figure 7). Therefore, the hit densities are simply the ratios of hit numbers (from table 4) and areas of the Endcap and Barrel sensitive layers, respectively. For the Tracker Endcap, the hit density is 7×10^{-4}/cm^2/bunch or 0.02/mm^2/train. For the Tracker Barrel, the hit density is 4×10^{-5}/cm^2/bunch or 0.001/mm^2/train. The tunnel background (no spoiler case) in the SiD tracker is also lower than the acceptable levels as defined in ref. [14].

There are two estimates of the acceptable background levels in the SiD muon system [12]. The RPCs (sensitive media) need 1 ms to re-charge a 1 cm^2 area around the avalanche. Therefore, the background rates of the order of 100 Hz/cm^2 would result in an unmanageable dead time. A radial hit distribution in the Muon Endcap is shown in figure 8. There are 14100 bunches/s, thus the tunnel background rate in the Muon Endcap (without spoilers) is about 400 Hz/cm^2, four times larger than the acceptable level [12]. The other limit (1 muon/cm^2/s) was presented as a conservative expert estimate [12]. A radial muon distribution at the Muon Endcap entrance is presented in figure 9. The tunnel backgrounds (without spoilers) exceed this level about four times.

If the detector sensitivity window is less than the time between the bunches, it is possible to use the difference in the signal and background timing to increase the signal/background ratio. Time distributions of hits in the muon system are presented in figure 10–11. The similar distributions for
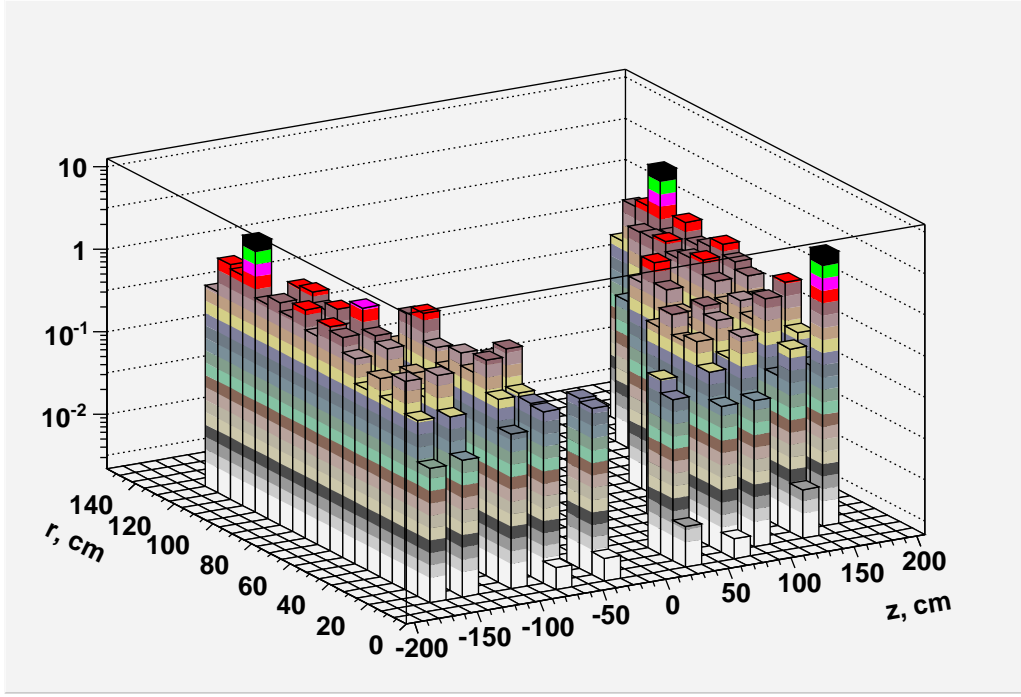
Figure 7. RZ distribution of hits per bunch in Tracker Endcap. No spoilers. Background is created by particles coming from positron tunnel only.
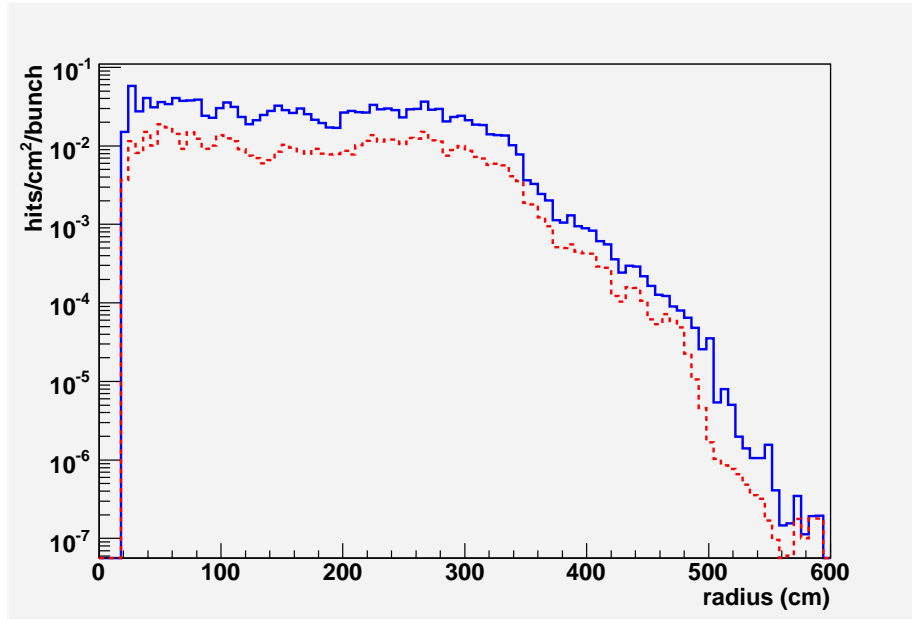

Figure 8. Radial distribution of hits in Muon Endcap. Solid line - total background, dashed line - background after bunch crossing. No spoilers. Particles coming from electron and positron tunnels are included.

all SiD sub-systems are presented in our preliminary report [16]. The time of a bunch crossing is chosen to be zero for these plots. A sub-detector starts collecting signals after a bunch crossing. Background hits produced before crossing do not count. The hits created by the tunnel background after a bunch crossing are presented in table 8 together with the total rates. The machine back-
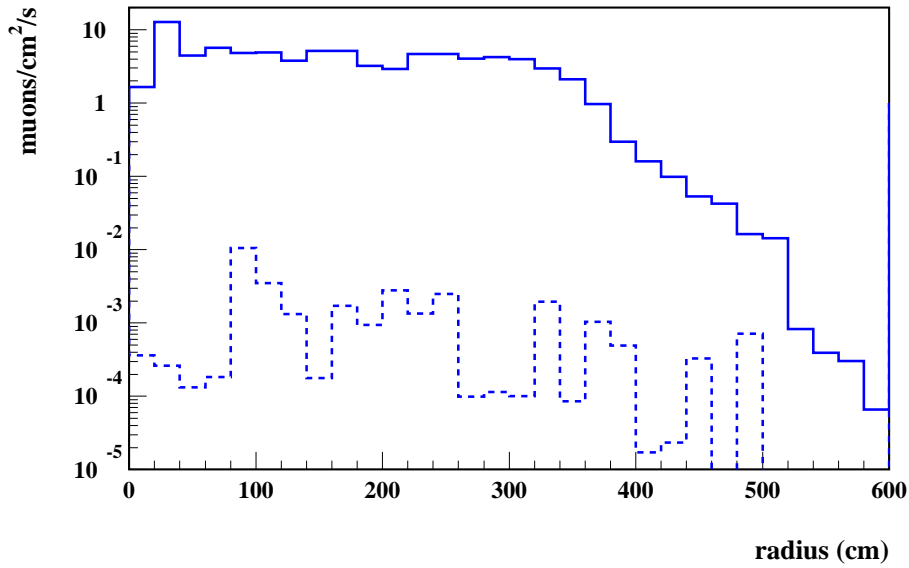
Figure 9. Radial distribution of muons at the Muon Endcap entrance. Solid line - no spoilers, dashed line - tunnel with spoilers. Muons coming from electron and positron tunnels are included.

ground after a bunch crossing is about twice lower than the total for the subsystems where muons dominate. Time window could be a very effective suppressor of background for the barrels (Muon Barrel, Hcal Barrel, Ecal Barrel). Note again that figures 1, 3–7, 10–11 and tables 2–6 present the machine background coming from the positron side only. About the same number of background particles comes from the electron side. Estimates of the occupancy (table 7), comparison of background levels and tolerable limits in the muon system and tracker are performed for particles coming from the both sides.

The machine-related backgrounds are calculated in this study for the positron beam coming to the IP. The muon fluxes here are slightly higher than for the electron-beam side, because of extra annihilation $e^+e^- \rightarrow \mu^+\mu^-$ at the very beginning of shower development in the collimators. A cross-section of the above annihilation process is proportional to the atomic charge Z. A cross section of muon pair production in γA interactions (Bethe-Heitler processes — the dominant source of muon fluxes at the detector) rises as Z^2. The annihilation contribution to background is practically negligible for copper and titanium collimators considered in this report. The difference between the positron and electron side backgrounds will be more significant for collimators made of low-Z materials.

6. Backgrounds and detector performance

Backgrounds affect ILC detector performance in three major ways: detector radiation aging, reconstruction of background objects (for example, tracks) not related to products of e^+e^- interactions, and deterioration of detector resolution (for example, jets energy resolution due to extra energy from background hits). Detailed simulations (beyond calculations presented in this paper) of the detector response to particles from primary e^+e^- collisions as well as other sources of backgrounds

	no spoilers	no spoilers	with spoilers	with spoilers
	total	after BC	total	after BC
	hits/bunch	hits/bunch	hits/bunch	hits/bunch
Muon Endcap	9422	3646	4.76	2.7
Muon Barrel	98	48	0.045	0.018
Hcal Endcap	1168	512	0.642	0.341
Hcal Barrel	628	322	0.148	0.060
Ecal Endcap	870	404	2.56	2.046
Ecal Barrel	200	102	0.82	0.806
FEcal Endcap	24	13.4	$1.1 \cdot 10^{-4}$	$5.9 \cdot 10^{-4}$
Tkr Endcap	158	84	21	16.89
Tkr Barrel	40	34	8	8
Vtx Endcap	$1.3 \cdot 10^{-2}$	$1.3 \cdot 10^{-2}$	3.2	3.2
Vtx Barrel	$1.1 \cdot 10^{-2}$	$1.1 \cdot 10^{-2}$	1.6	1.6
Luminosity Monitor	72	39.4	72	20

Table 8. Tunnel background in SiD sub-detectors, total and after bunch crossing (BC) taking into account both electron and positron sides.
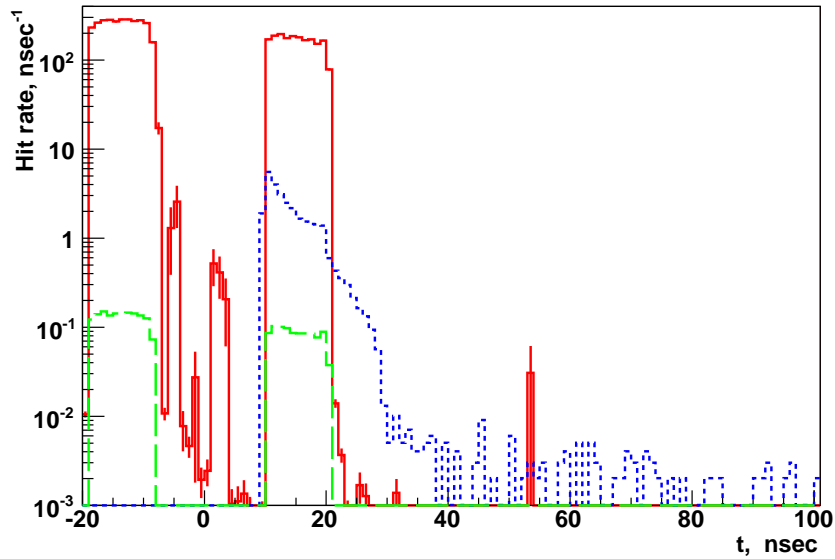

Figure 10. Time distribution of hit rates in Muon Endcap. Solid line - BDS background (no spoilers), dashed line - BDS background with spoilers, dotted line - e^+e^- events. BDS background is from positron tunnel only.

are needed in order to select final configuration of the BDS, including shielding, and to optimize detector performance.

Analysis of fluxes presented on figure 6 demonstrates that tunnel backgrounds provide large number of extra hits in the muon detectors, while in other detectors backgrounds from the IP dominate. Still, even without magnetic spoilers, background muon fluxes are within tolerable levels
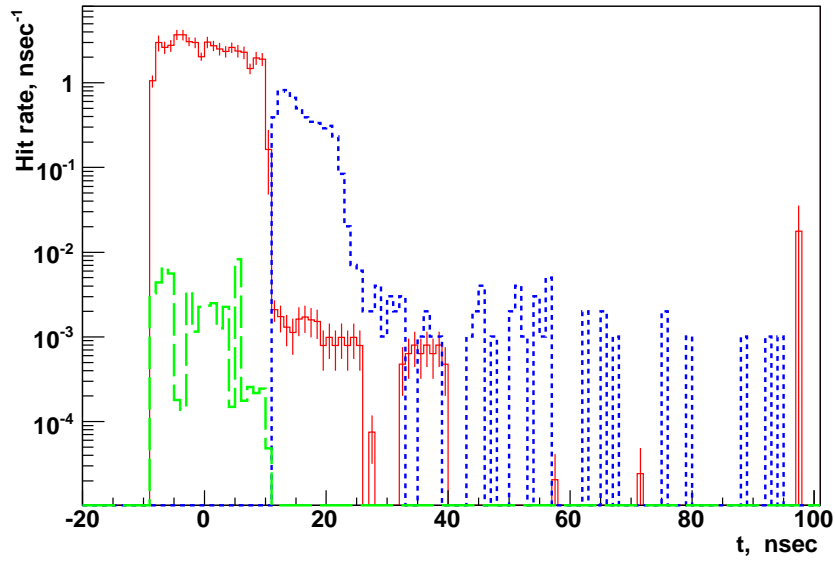
Figure 11. Time distribution of hit rates in Muon Barrel. Solid line - BDS background (no spoilers), dashed line - BDS background with spoilers, dotted line - e^+e^- events. BDS background is from positron tunnel only.

for muon detectors designed for modern collider experiments [17]. With magnetic iron spoilers, the BDS-related backgrounds in all SiD detectors become well below the IP and e+e- interaction backgrounds improving detector longevity and performance. Note that another essential function of the tunnel spoilers is to reduce radiation levels in a second experimental hall where construction work on a second collider detector can be underway while the ILC beams are on.

7. Conclusions

Detailed calculations of the background fluxes in the SiD detector components for ILC parameters from [11] and assumption of 0.1% beam loss in BDS are presented in this paper. Background flux distributions *vs* distance to the beam pipe, type of the particle creating energy deposition and timing of the hits with respect to the bunch crossing are presented. These studies provide important information for ILC detector designers opening options to reduce backgrounds by appropriate selection of detector properties, such as sensitivity to different types of particles and timing characteristics of the detectors. Option of reducing muon fluxes on the ILC detector by installing magnetic iron spoilers in the BDS tunnel is discussed. Such spoilers will reduce background muon fluxes on the ILC detector components to the level well below backgrounds from the IP region and e^+e^- collisions.

Acknowledgments

References

[1] N.V. Mokhov, A.I. Drozhdin and M.A. Kostin, *Beam collimation and machine-detector interface at the International Linear Collider*, Proceeding of PAC2005 Conf, 2995, Fermilab-Conf-05/154 (2005).

[2] N.V. Mokhov, *Backgrounds in ILC Detectors*, and *Beamline background muons in ILC detectors*, Proceeding of 2005 ILC Physics and Detector Workshop, SLAC-R-772 eConf:C0508141.

[3] J.E. Brau, M. Breidenbach and Y. Fujii, *The silicon detector (SiD) and linear collider detector R&D in Asia and North America*, SLAC-PUB-11413, DESY-04-123GH (2004).

[4] A.I. Drozhdin et al., *Comparison of the TESLA, NLC and CLIC beam-collimation system performance*, Fermilab-TM-2200 (2003), TESLA Report 2003-02 (2003).

[5] D. Angal-Kalinin et al., *ILC beam delivery WG summary: optics, collimation and background*, Fermilab-Conf-06-230-AD, SLAC-PUB-11629 (2006).

[6] J. Carter et al., *Simulation of the ILC collimation system using BDSIM, MARS15 and STRUCT*, Fermilab-Conf-06-219-AD (2006).

[7] I.S. Baishev, A.I. Drozhdin, N.V. Mokhov, *STRUCT Program User's Reference Manual*, SSCL-MAN-0034 (1994), http://www-ap.fnal.gov/users/drozhdin/.

[8] N.V. Mokhov, *The MARS Code System User's Guide*, Fermilab-FN-628 (1995);
N.V. Mokhov, K.K. Gudima, C.C. James et al, *Recent enhancements to the MARS15 code*, Fermilab-Conf-04/053 (2004), http://www-ap.fnal.gov/MARS/.

[9] L. Keller, *Muon background in a 1-TeV linear collider*, SLAC-PUB-6385 (1993).

[10] J. McCormic, *Full detector simulation using SLIC and LCDD*, Proceeding of 2005 ILC Physics and Detector Workshop, SLAC-R-772 eConf:C0508141.

[11] N. Walker, N. Phinney and K. Yokoya, *GG1 summary*, Proceeding of 2005 ILC Physics and Detector Workshop, SLAC-R-772 eConf:C0508141.

[12] T. Maruyama, *Backgrounds*, Proceeding of 2005 ILC Physics and Detector Workshop, SLAC-R-772 eConf:C0508141.

[13] T. Sjöstrand et al., *High-energy-physics event generation with PYTHIA 6.1*, Comput. Phys. Commun. **135** (2001) 238.

[14] W. Kozanecki et al., *Normalized background tolerance levels in ILC tracking detectors*, Proceeding of 2005 ILC Physics and Detector Workshop, SLAC-R-772 eConf:C0508141.

[15] R. Lemrani et al., *Low energy neutron propagation in MCNPX and GEANT4*, hep-ex/0601030.

[16] D.S. Denisov et al., *Machine-Related Background in the SiD detector at ILC*, FERMILAB-FN-0790-AD (2006).

[17] V.M. Abazov et al., *The upgraded DØ detector*, Nucl. Instrum. Meth. **A 565** (2006) 463.